◆ Human Brain Mapping 30:3009–3019 (2009) ◆

A Multiparametric Evaluation of Regional Brain Damage in Patients With Primary Progressive Multiple Sclerosis

Antonia Ceccarelli,[1] Maria A. Rocca,[1,2,3] Paola Valsasina,[1] Mariaemma Rodegher,[3] Elisabetta Pagani,[1] Andrea Falini,[2,4] Giancarlo Comi,[3] and Massimo Filippi[1,2,3]*

[1]*Neuroimaging Research Unit, Scientific Institute and University Ospedale San Raffaele, Milan, Italy*
[2]*CERMAC, Scientific Institute and University Ospedale San Raffaele, Milan, Italy*
[3]*Department of Neurology, Scientific Institute and University Ospedale San Raffaele, Milan, Italy*
[4]*Department of Neuroradiology, Scientific Institute and University Ospedale San Raffaele, Milan, Italy*

Abstract: The purpose of this study is to define the topographical distribution of gray matter (GM) and white matter (WM) damage in patients with primary progressive multiple sclerosis (PPMS), using a multiparametric MR-based approach. Using a 3 Tesla scanner, dual-echo, 3D fast-field echo (FFE), and diffusion tensor (DT) MRI scans were acquired from 18 PPMS patients and 17 matched healthy volunteers. An optimized voxel-based (VB) analysis was used to investigate the patterns of regional GM density changes and to quantify GM and WM diffusivity alterations of the entire brain. In PPMS patients, GM atrophy was found in the thalami and the right insula, while mean diffusivity (MD) changes involved several cortical-subcortical structures in all cerebral lobes and the cerebellum. An overlap between decreased WM fractional anisotropy (FA) and increased WM MD was found in the corpus callosum, the cingulate gyrus, the left short temporal fibers, the right short frontal fibers, the optic radiations, and the middle cerebellar peduncles. Selective MD increase, not associated with FA decrease, was found in the internal capsules, the corticospinal tracts, the superior longitudinal fasciculi, the fronto-occipital fasciculi, and the right cerebral peduncle. A discrepancy was found between regional WM diffusivity changes and focal lesions because several areas had DT MRI abnormalities but did not harbor T2-visible lesions. Our study allowed to detect tissue damage in brain areas associated with motor and cognitive functions, which are known to be impaired in PPMS patients. Combining regional measures derived from different MR modalities may be a valuable tool to improve our understanding of PPMS pathophysiology. *Hum Brain Mapp 30:3009–3019, 2009.*

Key words: primary progressive multiple sclerosis; voxel-based; regional; gray matter; atrophy; white matter; diffusion tensor; magnetic resonance imaging

Contract grant sponsor: Fondazione Italiana Sclerosi Multipla (FISM); Contract grant number: 2003/R/48.

*Correspondence to: Dr. Massimo Filippi, Neuroimaging Research Unit, Department of Neurology, Scientific Institute and University Ospedale San Raffaele, Via Olgettina, 60, 20132 Milan, Italy.
E-mail: m.filippi@hsr.it

Received for publication 25 June 2008; Revised 27 October 2008; Accepted 4 December 2008

DOI: 10.1002/hbm.20725

Published online 26 January 2009 in Wiley InterScience (www.interscience.wiley.com).

INTRODUCTION

Patients with the primary progressive (PP) form of the disease represent about 10–15% of the general multiple sclerosis (MS) patient population [Miller and Leary, 2007]. PPMS is characterized, clinically, by a progressive worsening of symptoms/signs from the onset of the disease without phases of remission [Filippi et al., 2004; Polman et al., 2005; Thompson et al., 2000].

Several magnetic resonance imaging (MRI) studies of the brain and cord have shown that the extent of overall central nervous system (CNS) damage in these patients in terms of macroscopic T2-hyperintense, T1-hypointense, and gadolinium-enhancing lesions is similar, if not less pronounced, than that observed in other, and usually less disabling, disease phenotypes [Filippi et al., 2004; Ingle et al., 2002; Miller and Leary, 2007]. During the past decades, the application of quantitative, MR-based techniques, including magnetization transfer (MT) MRI, diffusion tensor (DT) MRI, and proton MR spectroscopy (^{1}H-MRS), for the assessment of microscopic tissue damage in these patients has revealed the presence of a diffuse damage to the normal-appearing tissues, including not only the white matter (WM) but also the gray matter (GM) [De Stefano and Filippi, 2007; Filippi et al., 2000; Rocca et al., 2003; Rovaris et al., 2001, 2002, 2005a,b, in press] and the spinal cord [Agosta et al., 2005, 2006, 2007; Rovaris et al., 2001, in press]. Despite these results, the factors responsible for the adverse clinical course of patients with PPMS are not fully elucidated yet.

In this study, we wished to take advantage from recent technical developments to gain additional insights into the MRI substrates of PPMS, which might ultimately lead to disability accumulation in these patients. For this, we used a high-field MR scanner and parallel imaging technology, which, thanks to an increased spatial resolution and signal-to-noise ratio (SNR) [Charil et al., 2006], are contributing to improve the sensitivity of MRI for detecting CNS damage. This latter aspect is particularly important for diffusion tensor (DT) MRI, because the application of diffusion gradients causes an attenuation of the signal, which in turn intrinsically limits the SNR available. The recent application of DT MRI at 3 Tesla (T) for the quantification of damage of the different brain compartments has confirmed the potential of such a strategy in the assessment of patients with MS [Ceccarelli et al., 2007, 2008]. We also applied a voxel-based (VB) approach [Ashburner and Friston, 2000], which allows to define reliably the topography of damage in the brain WM and GM. Indeed, using VB morphometry (VBM), previous studies have shown that regional GM atrophy is restricted to the deep GM (especially the thalamus), in patients with early PPMS, while cortical and infratentorial GM structures are involved later on, when the disease progresses [Khaleeli et al., 2007; Sepulcre et al., 2006]. An uneven distribution of disease-related damage in the different brain compartments might help to explain some of the clinical manifestation of the disease, thus contributing to solve, at least partially, the clinical-radiological paradox.

Finally, we used a multiparametric approach, based on the combination of pieces of information derived from different MR modalities, that is, brain volumetry and diffusivity because a few preliminary studies [Galanaud et al., 2003; Iannucci et al., 2001; Mainero et al., 2001] on 1.5 T scanners showed that this might represent an ideal strategy for an accurate in vivo imaging of the two main pathological aspects of MS damage (i.e., the amount of tissue lost and the status of the remaining tissues). Furthermore, the assessment of regional changes of DT and volumetry measures might allow to identify brain regions more sensitive to disease-related damage, which might be the target for future treatment trials.

The main hypotheses of this study were that diffuse structural brain abnormalities are frequent and overcome focal T2 lesions in PPMS, and that the use of various MR-based techniques might contribute to define the distribution of the involvement of the different brain compartments at a regional level.

MATERIALS AND METHODS

Subjects

We recruited 18 patients with PPMS [Polman et al., 2005] (10 women and 8 men, mean age [range] = 49.6 [38–73] years, median [range] expanded disability status scale [EDSS] [Kurtzke, 1983] score = 5.5 [3.0–7.0], mean disease duration [range] = 10.7 [4–21] years). All patients were evaluated clinically by the same experienced neurologist, who was blinded to the MRI results, on the same day of MR examination. Seventeen sex- and age-matched (11 women and 6 men; mean age 51.3 years, range 26–68 years) healthy volunteers with no history of neurological disorders were also studied. The study was approved by the local Ethics Committee, and a written informed consent was obtained from all subjects prior to study entry.

MRI Acquisition

Brain MR scans were obtained using a 3.0 T scanner (Intera, Philips Medical Systems, Best, The Netherlands). During a single imaging session, the following sequences were obtained from all subjects: (1) dual-echo turbo spin echo (TSE) sequence (TR = 3,500, TE = 24/120 ms; echo train length = 5; flip angle = 150°, 44 contiguous, 3-mm-thick, axial slices with a matrix size = 256 × 256 and a field of view [FOV] = 240 × 240 mm^2); (2) 3D T1-weighted fast field echo (FFE) sequence (TR = 25, TE = 4.6 ms, flip angle = 30°, 220 contiguous, axial slices with voxel size = 0.89 mm × 0.89 × 1 mm, matrix size = 256 × 256, FOV = 230 × 230 mm^2); (3) pulsed-gradient spin-echo echo planar pulse sequence with SENSE (acceleration factor = 2.5, TR = 8283.2, TE = 80; 55, 2.5 mm thick axial slices; acquisition matrix size = 96 × 96; FOV = 240 × 240 mm^2; after

SENSE reconstruction, the matrix dimension of each slice was 256 × 256, with an in-plane pixel size of 0.94 × 0.94 mm) and diffusion gradients applied in 35 noncollinear directions, using a gradient scheme, which is standard on this system (gradient over-plus) and optimized to reduce echo time as much as possible. Two optimized b factors were used for acquiring diffusion weighted images (b_1 = 0, b_2 = 1,000 sec/mm^2). Fat saturation was performed to avoid chemical shift artifacts. All slices were positioned to run parallel to a line that joins the most infero-anterior and infero-posterior parts of the corpus callosum (CC).

Image Analysis and Postprocessing

The structural MRI postprocessing was performed by a single experienced observer, unaware to whom the scans belonged. Total T2 lesion volumes (LV) were measured using a local thresholding segmentation technique (Jim 4.0, Xinapse System, Leicester, UK).

Global assessment of volumes and DT MRI changes of the NAWM and GM

On 3D-FFE images, normalized brain volumes (NBV) and intracranial volume (ICV) were measured using the cross-sectional version of the fully automated structural imaging evaluation of normalized atrophy (SIENAx) software [Smith et al., 2001].

Diffusion gradient directions were corrected for scanner settings (i.e., slice angulation, slice orientation, etc.) before DT estimation [Farrell et al., 2007]. From DT MR images, mean diffusivity (MD) and fractional anisotropy (FA) maps were derived [Pierpaoli and Basser, 1996] and average MD of the normal appearing (NA) WM, and GM, and average FA of the NAWM were computed, as previously described [Ceccarelli et al., 2007]. Average FA was derived only for the NAWM as no preferential direction of water molecular motion is expected to occur in the GM because of the absence of a microstructural anisotropic organization of this tissue compartment.

Assessment of topographical distribution of atrophy and DT MRI changes of the WM and GM

Regional volumetry analysis was performed on 3D T1-weighted FFE images using VBM and statistical parametric mapping (SPM2) software (www.fil.ion.ucl.ac.uk/spm). An optimized VBM method was used, as described by Good et al. [2001]. Briefly, a customized T1 template, together with the corresponding probability maps of GM, WM, and cerebrospinal fluid (CSF), was first created using 3D-FFE scans of both controls and MS patients. Then, GM probability maps in the native space were normalized toward the new customized GM template, and the computed transformation was used to modulate the normalized GM maps, to incorporate the point-wise volume expansion/contraction induced by the transformation [Ashburner and Friston, 2000].

To assess GM regional diffusivity changes, the nonlinear transformation previously calculated was applied to the MD maps coregistered onto the 3D-FFE with a rigid transformation. To assess MD and FA regional changes in the WM, MD and FA maps were normalized into the standard SPM space. Using SPM2, a rigid transformation was calculated between the nondiffusion weighted images and the T2-weighted images and between the T2-weighted images and the SPM T2-weighted atlas. The transformation was then applied to the FA maps. A customized FA atlas was obtained by averaging the transformed FA maps of both controls and MS patients. Then, a nonlinear transformation was calculated between the customized FA atlas and the FA maps and applied to the MD maps. GM modulated maps, WM FA and MD maps and GM MD maps were all smoothed with a 12 mm^3 FWHM Gaussian kernel in the MNI space, before their use as input for the statistical analysis.

To avoid MS lesion misclassification, lesions were masked out from the GM maps and reassigned to WM maps, after each segmentation step of the described postprocessing strategy. To this end, a lesion mask of the T2-visible lesions was created, coregistered to the 3D-FFE space and normalized to the MNI space. To exclude from the statistical analysis pixels assigned by the segmentation to GM/WM with low probability values and pixels with a low inter-subject anatomical overlay after normalization, GM and WM masks were created by averaging GM and WM normalized maps from all subjects. These masks were eroded (erosion of the first-line outer voxels), thresholded at a value of 0.50 (pixels with computed GM fraction values >50% were selected) and then used as explicit mask during the statistical analysis.

From controls' data, a study-specific tractography atlas was created [Pagani et al., 2005], using a tractography algorithm to construct the major intra- and inter-hemispheric WM fiber bundles, including the corticospinal tract (CST), the CC, the optic radiation (OR), the superior longitudinal fasciculus (SLF), the fronto-occipital fasciculus (FOF), the uncinate fasciculus, and the fornix. Then, to assess the location of regions of atrophy and DT MRI changes of the previous WM fiber bundles, SPM maps resulting from regional analysis of atrophy and DT MRI WM and GM changes were superimposed to WM fibers bundle probability maps [Pagani et al., 2005].

Areas of anatomical correspondence between regional GM and WM damage

Assessment of areas of anatomical correspondence between decreased WM FA and increased WM MD changes, as well as between GM loss and increased GM MD, were identified by overlaying the results of the corresponding analysis on the same anatomical image (FA atlas).

Spatial distribution of T2-visible lesions

A probability map of the spatial distribution of T2-visible lesions was also created for PPMS patients by averaging the normalized T2-lesion masks previously created. This map was superimposed to the SPM maps of DT MRI WM and GM changes.

Statistical Analysis

A Mann-Whitney test was used to assess between-group differences in demographic and MRI measures of global NAWM and GM damage.

An analysis of covariance (ANCOVA) was used to compare volumetry and diffusivity measurements between PPMS patients and controls. Age, sex, and ICV volume were included as nuisance covariates for the volumetry comparisons, whereas age and sex were used as nuisance covariates for the diffusivity comparisons. We used a false-discovery rate (FDR) correction at $P < 0.001$ for multiple comparisons at voxel level across the whole brain. In addition, only clusters with 10 or more contiguous voxels were considered.

A linear regression analysis was used to assess the correlations between regional damage and clinical findings (EDSS and disease duration). Age, sex, and ICV volume were included as nuisance covariates for the volumetry correlations, whereas age and sex were used as nuisance covariates for the diffusivity correlations. The significance threshold was set at $P < 0.001$ (uncorrected for multiple comparisons).

RESULTS

Volumetry and Diffusivity Changes of Overall NAWM and GM

In Table I, brain volumetry and DT-MRI derived metrics from controls and PPMS patients are reported. Except for NAWM average MD, all DT-MRI derived metrics were significantly different between PPMS patients and controls (P values ranging from < 0.0001 to 0.04).

Regional Distribution of Atrophy and Diffusivity Changes of the GM and WM

GM atrophy

Compared to controls, PPMS patients had significant clusters of locally reduced GM concentration in the thalami (SPM space coordinates: right thalamus 3, −11, 4; left thalamus −2, −4, 3; t values = 5–14 for both), and the right insula (SPM space coordinates: 41, −17, 12; t value = 4.56) ($P < 0.05$, corrected for multiple comparisons) (see Fig. 1].

TABLE I. Brain volumetric and DT MRI derived metrics of the normal appearing white and gray matter from healthy volunteers and patients with primary progressive multiple sclerosis (PPMS)

	Healthy volunteers	PPMS	P[a]
T2 LV (SD) (ml)	0.98 (2.3)	9.5 (12.0)	<0.0001
NBV (SD) (ml)	1602.3 (100.4)	1533.8 (86.5)	0.05
Average lesion FA (SD)	0.32 (0.06)	0.34 (0.05)	n.s.
Average lesion MD (SD)	0.93 (0.08)	1.06 (0.09)	0.002
NAWM Average FA (SD)	0.38 (0.02)	0.36 (0.03)	0.001
NAWM Average MD (SD)	0.78 (0.03)	0.80 (0.05)	n.s.
GM Average MD (SD)	0.91 (0.03)	0.97 (0.09)	0.04

[a] Mann-Whitney Test. See text for further details.
PPMS, primary progressive multiple sclerosis; NBV, normalized brain volume; NAWM, normal-appearing white matter; GM, gray matter; SD, standard deviation; MD, mean diffusivity; FA, fractional anisotropy.
Average MD is expressed in units of $mm^2s^{-1} \times 10^{-3}$, FA is a dimensionless index.

GM MD changes

Compared to controls, PPMS patients had significant clusters of locally increased GM MD in several cortical-subcortical structures, including the left middle frontal gyrus (MFG), the cingulate gyri, the left inferior parietal lobe (IPL), the left superior temporal gyrus (STG), the middle temporal gyri (MTG), the inferior frontal gyri (IFG), the lingual gyri (LG), the left precuneus, the right cuneus, and bilaterally in the cortex of the posterior lobe of the cerebellum, the insula, the thalamus, and the caudate nucleus (Table II, Fig. 1).

Areas of anatomical correspondence between GM loss and GM MD changes

In PPMS patients, an overlap between GM loss and increased GM MD was found exclusively in the thalami (see Fig. 1).

WM FA changes

Compared to controls, PPMS patients had significant clusters of locally decreased WM FA in several regions of the frontal and temporal lobes, the CC, the cingulum, the ORs, and the middle cerebellar peduncles (Table III, Fig. 2].

WM MD changes

Compared to controls, PPMS patients had significant clusters of locally increased WM MD in several short associative fibers in all cerebral lobes, bilaterally, as well as in the anterior and posterior limbs of the internal capsulae, the CC, the SLFs, the FOFs, the CSTs, the ORs, the right

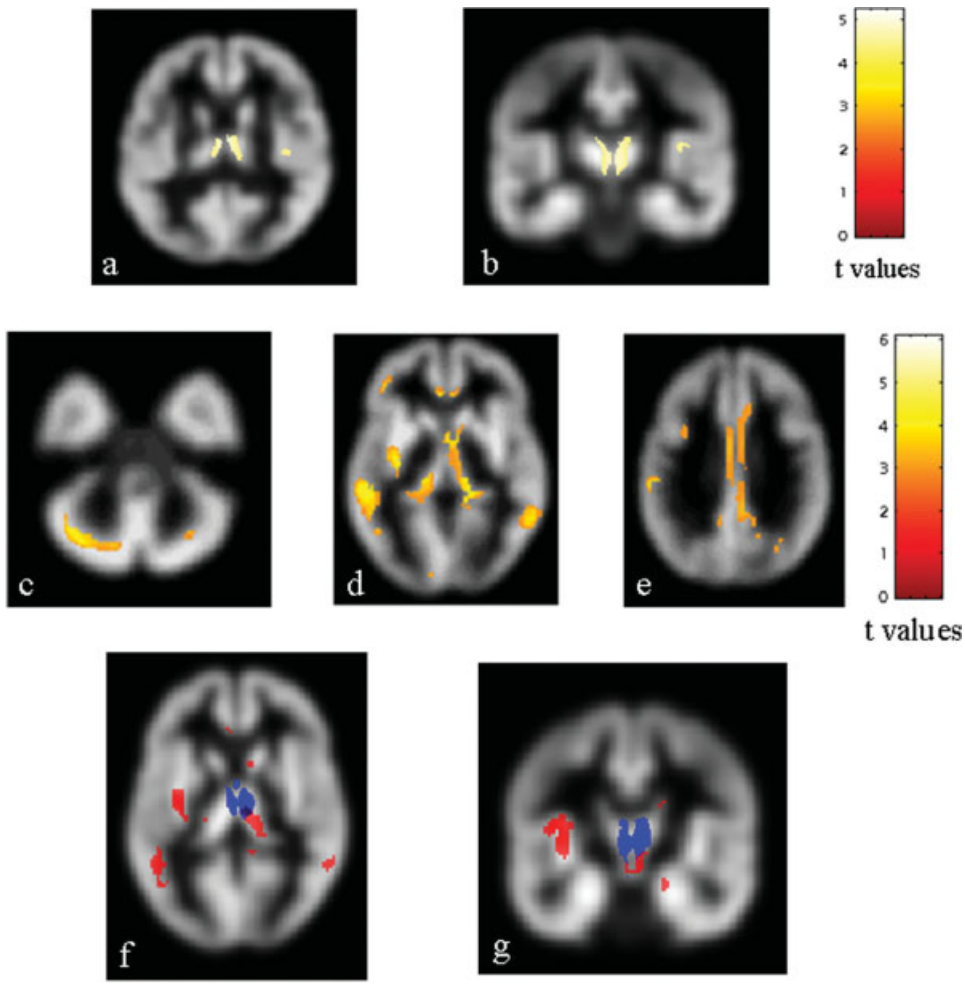

Figure 1.

Top row: statistical parametric mapping (SPM) regions (color-coded for *t* values) with decreased gray matter (GM) concentration in patients with primary progressive multiple sclerosis (PPMS) compared with controls ($P < 0.05$, corrected for multiple comparisons). The thalami and the right insula appear to be damaged (**A**, **B**). Middle row: SPM regions (color-coded for *t* values) with increased GM mean diffusivity (MD) in PPMS patients compared with controls ($P < 0.001$, FDR corrected). Several cortical-subcortical structures, including the left middle frontal gyrus (MFG) (**D**), the cingulate gyri (**E**), the left inferior parietal lobe (IPL) (**E**), the left superior temporal gyrus (STG) (D), the middle temporal gyri (MTG) (D), the inferior frontal gyri (IFG) (D), the lingual gyri (LG) (D), the left precuneus (E), the right cuneus (D), the cerebellum, bilaterally (C), the insulae (D), the thalami (D), and the caudate nuclei (D) appear to be damaged. Bottom row: SPM regions with anatomical correspondence between GM atrophy (blue) and GM MD (red) changes. An overlap is visible in the thalami (**F**, **G**). Images are in neurological convention. See text for further details.

cerebral peduncle and the middle cerebellar peduncles (Table IV, Fig. 2).

Areas of anatomical correspondence between decreased WM FA and increased WM MD changes

In PPMS patients, an overlap between decreased WM FA and increased WM MD was found in the CC, the cingulate gyrus, the left short temporal fibers, the right short frontal fibers, the ORs, and the middle cerebellar peduncles (see Fig. 2).

Analysis of Regional Distribution of T2-Visible Lesions

To investigate the correspondence between areas of MD and FA changes and areas with an increased occurrence of lesions, lesion maps were superimposed onto the MD and

TABLE II. Regions of significantly increased gray matter mean diffusivity in patients with primary progressive multiple sclerosis (PPMS) compared to controls ($P < 0.001$)

	PPMS vs controls			
Anatomical regions	Side	BA	SPM coordinates	*t* value
Middle frontal gyrus	L	47	−40, −42, −4	4.45
	L	9	−36, 8, 36	3.99
Cingulated gyrus	R	32	6, 30, 22	4.84
	R	29	6, −42, 20	4.52
	L	32	−4, 26, −6	4.23
Insula	R	13	46, 8, 6	3.81
	L	13	−34, −14, 6	5.50
Thalamus	R	–	14, −24, 2	4.73
	L	–	−12, −26, −6	4.85
Caudate nucleus	R	–	6, 4, −6	6.08
	L	–	−2, 6, −8	5.18
Inferior parietal lobe	L	40	−54, −46, 22	4.58
	L	40	−60, −26, 32	4.53
Superior temporal gyrus	L	42	−56, −14, 12	4.58
	L	41	−54, −23, 5	4.06
Middle temporal gyrus	R	21	60, −52, 2	4.67
	L	22	−58, −38, −6	5.67
Inferior temporal gyrus	R	30	42, −50, −16	4.00
	L	20	−50, −52, −14	5.04
	L	35	−16, –18, −18	4.71
Lingual gyrus	R	19	30, −60, −6	4.24
	L	17	−12, −92, −4	4.15
Precuneus	L	31	−12, −54, 28	3.84
Cuneus	R	31	22, −56, 22	4.09
	R	18	8, −82, 22	3.96
Cerebellum	R	–	32, 66, −40	4.08
	R	–	2, −74, −20	3.96
	L	–	−16, −76, −40	4.44

PPMS, primary progressive multiple sclerosis; R, right; L, left; BA, Brodman area.
See the text for further details.

FA WM SPMt maps. This analysis showed a discrepancy between regional WM FA and MD changes and focal lesion distribution, as several areas were identified that had DT MRI abnormalities, but did not harbor T2-visible lesions (see Fig. 3).

Correlations Between GM and WM Damage and Clinical Characteristics

No correlation was found between GM and NAWM structural MRI changes and the tested clinical variables.

DISCUSSION

In this study, we used a multiparametric VB approach to define the topographical distribution of tissue damage in the NAWM and GM in patients with PPMS, with the ultimate goal of gaining additional insight into the MRI correlates of this puzzling condition, where the small amount of focal lesion pathology clashes with the severe clinical status of the patients [Filippi et al., 2004; Ingle et al., 2002; Miller and Leary, 2007]. Several previous quantitative MR-based studies [Agosta et al., 2005, 2006, 2007; De Stefano and Filippi, 2006; Rocca et al., 2003; Rovaris et al., 2001, 2002, 2005a,b, in press] have demonstrated convincingly that PPMS patients have subtle and diffuse damage in the NA brain tissues, even if the nature of these changes is still poorly understood. In agreement with these studies [Rocca et al., 2003; Rovaris et al., 2002, 2005b], our analysis of DT MRI derived metrics of overall NAWM and GM confirmed the presence of diffuse extra-lesional changes in PPMS patients.

Assessment of Volumetry and Diffusivity Changes in the GM

The VBM analysis of GM atrophy demonstrated selective damage in the thalami, and the right insula in PPMS patients. Thalamic involvement in MS has been reported by both pathological [Brownell and Hughes, 1962; Cifelli et al., 2002] and imaging [Cifelli et al., 2002; Fabiano et al., 2003; Inglese et al., 2004, 2007; Ormerod et al., 1987; Wylezinska et al., 2003] studies. GM loss in the thalami seems to be an almost constant profile of MS, because it has been shown in patients with early PPMS [Khaleeli et al., 2007; Sepulcre et al., 2006], in those with early RRMS [Audoin et al., 2006], and in pediatric MS patients [Mesaros et al., 2008]. A recent VBM comparison of patients with different disease phenotypes [Ceccarelli et al., in press] hypothesized that tissue loss in the thalamus might be a prominent finding in patients with the progressive forms of MS, possibly as a result of a longer disease duration. The correlation found by the majority of studies [Cifelli et al., 2002; Fabiano et al., 2003; Inglese et al., 2004; Wylezinska et al., 2003] between thalamic GM loss and T2 LV supports retrograde neuroaxonal degeneration or anterograde transynap-

TABLE III. Regions of significantly decreased white matter fractional anisotropy in primary progressive multiple sclerosis (PPMS) patients compared to controls ($P < 0\ 001$)

	PPMS vs. controls		
Anatomical regions	Side	SPM coordinates	*t* value
Short frontal fibers	R	40, 40, −6	4.06
Short temporal fibers	L	−36, −58, 16	4.25
	L	−46, −34, −16	4.02
Corpus callosum	–	−6, 6, 30	3.82
	–	−16, −44, 16	3.64
	–	22, −42, 24	3.70
Cingulum	R	12, 36, −8	4.67
	L	−8, 32, –10	4.75
	L	−10, –48, 10	4.25
Optic radiation	R	30, −64, 24	4.81
	L	−28, −50, 18	4.14
Middle cerebellar peduncle	R	26, −66, −38	4.56
	L	−32, −62, −40	4.00

PPMS, primary progressive multiple sclerosis; R, right; L, left.
See the text for further details.

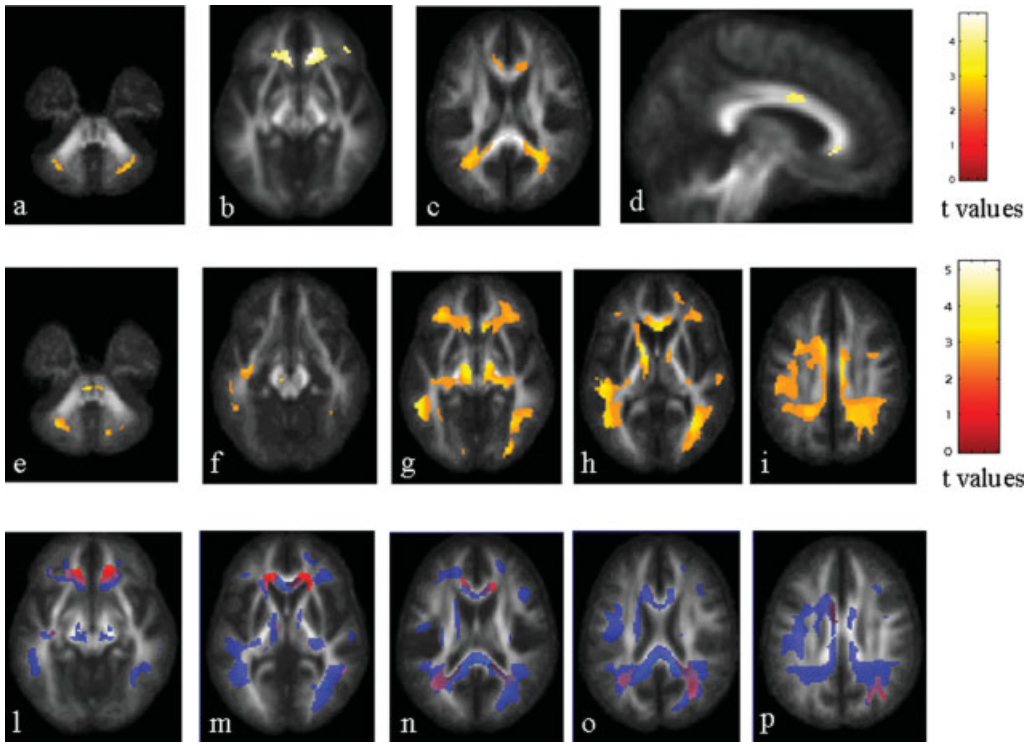

Figure 2.

Top row: statistical parametric mapping (SPM) regions (color-coded for *t* values) with decreased white matter (WM) fractional anisotropy (FA) values in patients with primary progressive multiple sclerosis (PPMS) compared with controls ($P < 0.001$, FDR corrected). Several regions in the frontal and temporal lobes, the CC, the cingulum, the OR, and the middle cerebellar peduncle, bilaterally, appear to be damaged. Middle row: SPM regions (color-coded for *t* values) with increased WM mean diffusivity (MD) in PPMS patients compared with control subjects ($P < 0.001$, FDR corrected). Widespread MD abnormalities in the major short and long intra-hemispheric associative pathways, as well in the CC and cingulum are visible. Bottom row: SPM regions with anatomical correspondence between decreased WM FA (red) and increased WM MD (blue). An overlap is visible in the CC, the cingulate gyrus, the left short temporal fibers, the right short frontal fibers, the OR, bilaterally, and the middle cerebellar peduncles. Images are in neurological convention. See text for further details.

tic changes from axonal transection in WM lesions as possible pathologic substrates of such a damage. Alternatively, thalamic damage might be the consequence of local inflammatory activity [Brownell and Hughes, 1962].

The insula has numerous connections with the cerebral cortex (frontal lobe, temporal lobe, parietal lobe and anterior cingulate cortex), the basal ganglia, the amygdala and other areas that are part of the limbic system, such as the parahippocampal cortex. As a consequence its involvement in PPMS patients might contribute to explain, at least in part, deficits of cognitive function often encountered in these patients [Camp et al., 2005].

The VB analysis of GM MD changes revealed the presence of widespread abnormalities, which extended well beyond those detected by the assessment of atrophy, and involved several cortical-subcortical regions, located in all cerebral lobes, the cerebellum, the insulae and the caudate nuclei. Each of these regions has a specific functional role, as a consequence their involvement might contribute to explain part of the symptoms typically experienced by these patients. For instance, a reduction of glucose metabolism in the hippocampus, thalamus, associative occipital cortex, and cerebellum has been associated with long-term memory deficits in MS patients [Paulesu et al., 1996]. The cerebellum has extensive connections with the motor and somatosensory cortex and is involved in motor programming, execution, and control [Ehrsson et al., 2002]. Recent studies have also highlighted its role in cognition [Schmahmann and Caplan, 2006; Schmahmann and Sherman, 1998].

The discrepancy between atrophy and DT MRI results confirms that these two techniques are sensitive toward different aspects of MS pathology and, as a consequence, might provide complementary pieces of information for the assessment of CNS damage in these patients. It is worth noting that the only regions that showed an overlap between MD and atrophy changes were the thalamus and the insula. Even if we can not completely rule out that

TABLE IV. Regions of significantly increased white matter mean diffusivity in patients with primary progressive multiple sclerosis (PPMS) compared to controls ($P < 0.001$)

	PPMS *vs.* controls		
Anatomical regions	Side	SPM coordinates	*T* value
Short frontal fibers	R	46, 18, 14	4.21
	L	–40, 16, 10	3.86
	L	–32, 38, –8	4.68
Short parietal fibers	R	10, –42, 12	5.11
	L	–46, –46, 26	3.69
	L	–44, –10, 16	4.58
Short temporal fibers	R	58, –18, 2	3.66
	R	42, 6, 12	3.55
	L	–32, 0, –30	3.91
Short occipital fibers	L	–12, –84, –6	3.55
Corpus callosum	–	2, 24, –2	4.83
	–	0, 0, 24	4.44
	–	–8, –40, 8	5.78
	–	10, –44, 18	5.25
	–	10, –42, 12	5.11
Anterior limb of internal capsule	R	10, 2, 0	4.05
	L	–12, 6, 4	5.60
Posterior limb of internal capsule	L	–12, 6, 4	5.60
Superior longitudinal fasciculus	R	32, –58, 0	4.58
	R	36, 0, 34	3.91
	L	–44, –10, 16	4.96
Fronto-occipital fasciculus	R	4, 24,10	4.82
	L	–44,–16,–14	4.20
Corticospinal tract	R	12, –6, –8	4.83
	L	–12, –16, –6	5.60
	L	–4, –32, –38	4.98
Optic radiation	R	28, –74, 18	4.68
	L	–56, –42, –6	5.23
Cerebral peduncle	R	30, –18, 16	3.48
Middle cerebellar peduncle	R	14, –70, –40	3.94
	L	–30, –64, –40	4.48

PPMS, primary progressive multiple sclerosis; R, right; L, left. See the text for further details.

these findings might be because of methodological issues (i.e., the small size of the sample studied), it is tempting to speculate that these results might be secondary to the "strategic" position of these structures in the brain, which in turn render them vulnerable to processes, such as Wallerian and transynaptic degeneration of fibers passing through diseased WM areas.

The notion that combining different MR modalities might be a valuable tool to improve the understanding of PPMS pathophysiology is also supported by the results of a recent voxel-based study in a relatively large sample of PPMS patients, which assessed GM volume and MT MRI changes in these patients and identified several cortical and subcortical regions with abnormalities of MT ratio (MTR) values, in the absence of significant atrophy changes [Khaleeli et al., 2007]. It is worth noting that in this previous study [Khaleeli et al., 2007], consistently with the major clinical manifestations of the disease, the largest and more significant regions of MTR and volume reduction were in the precentral gyrus, which did not appear to be involved in our study. Differences in number and clinical characteristics of the patients included as well different sensitivities of the MR methods applied toward the heterogeneous pathological substrates of MS are among the factors which might contribute to explain these discrepant results. In the VB analysis of regional distribution of GM damage, we applied several strategies to reduce possible technical biases on our results, including the masking of T2-visible lesions from the GM maps and the application of a GM mask during the statistical analysis (to exclude pixels with a low probability to belong to GM and those with a low inter-subject anatomical overlay). Furthermore, a stringent statistical threshold was used. As a consequence, our results are unlikely to represent false positive differences.

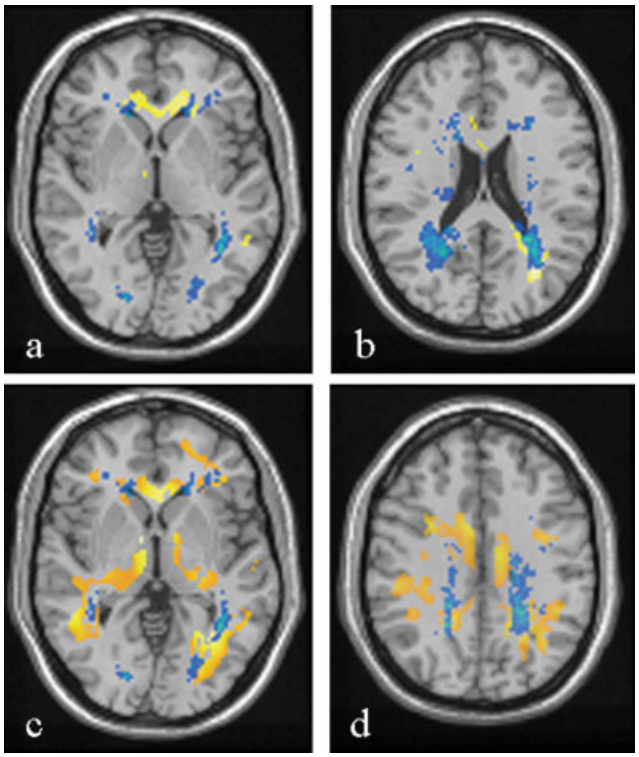

Figure 3.
Two representative axial slices showing lesion probability maps (in yellow) and areas with significant decreased fractional anisotropy (FA) (SPMt map in blue) for primary progressive multiple sclerosis (PPMS) (**A** and **B**). The overlap between lesion probability maps and areas with significant decreased FA are in light green. Two representative axial slices showing lesion probability maps (in yellow) and areas with significant increased mean diffusivity (MD) (SPMt map in blue) for PPMS (**C** and **D**). The overlap between lesion probability maps and areas with significant increased MD are in light green. Images are in neurological convention. See text for further details.

Assessment of Diffusivity Changes in the WM

The analysis of regional distribution of tissue damage in the WM showed the presence of diffuse, and predominantly bilateral, FA and MD abnormalities in several intra- and inter-hemispheric WM fiber bundles, including the CC, the cingulate gyrus, the short temporal fibers, the short frontal fibers, the OR, and the middle cerebellar peduncles. In addition, widespread MD abnormalities, not associated with corresponding FA changes, were detected in an additional set of WM pathways, which represent important nodes for somatosensory integration and for cognitive function, including the internal capsules, the CSTs, the SLFs, the FOFs, and the cerebral peduncles. The relation between damage of specific WM pathways and cognitive dysfunction in patients with MS is still poorly understood. Using a voxel based lesion function mapping, a recent study in MS patients with different clinical phenotypes [Sepulcre et al., 2008] has demonstrated an association between damage of specific pathways located in the temporal and frontal lobes as well as in the corticospinal tract and thalamus and performance on declarative verbal memory.

Several pathological substrates are likely to contribute to the observed WM diffusivity changes [Kutzelnigg et al., 2005; Lassmann et al., 2007]. Myelin and axonal loss should lead to increased MD (by causing a net loss of structural barriers), and reduced FA (by altering the physiological organization of structural barriers to water molecular motion). Reactive gliosis might also contribute to a decreased FA (glial cells do not have the same anisotropic morphology as the tissue they replace). The partial mismatch between MD and FA findings might also be secondary to the presence of inflammatory processes, which have been suggested to become trapped behind a closed or repaired blood-brain-barrier in the progressive forms of the disease [Lassmann et al., 2007].

As for GM analysis, we applied several strategies to minimize possible biases on our results, including the registration of individuals' FA maps to a FA atlas and not to the T2-weighted images (because WM fiber bundles are visualized better on FA maps), and the use of a conservative threshold to WM masks, to minimize the effect of partial volume from voxels containing CSF. In addition, to have a more precise location of DT MRI abnormalities, a study-specific WM fiber bundle atlas of the major WM pathways was also built.

Assessment of Regional Distribution of T2-Visible Lesions

To improve the understanding of the mechanisms responsible for the patterns of regional distribution of WM damage in patients with PPMS, we investigated the location of T2-visible lesions and analyzed the correlation between the distribution of T2-visible lesions and that of FA and MD WM damage. This analysis showed a partial discrepancy between regional WM FA and MD changes and lesion distribution, as several areas were identified that had DT MRI abnormalities (mainly increased MD values) and no T2-visible lesions. These results confirm previous imaging [Rocca et al., 2003] and pathological [Lassman et al., 2007] findings suggesting that diffuse NAWM damage, beyond macroscopic T2-visible lesions, is likely to have a prominent role in the pathogenesis of PPMS.

Correlations Between GM and WM Damage and Clinical Characteristics

Disappointingly, we found no correlation between regional damage in the NAWM and GM and clinical metrics, such as disability and disease duration. Several factors can contribute to explain such a finding. First, we focused our investigation on the distribution of regional damage in different brain compartments and we did not consider the involvement of the spinal cord, which may play a major role in locomotor disability in PPMS [Agosta et al., 2005, 2007; Rovaris et al., 2001, in press]. Second, we used only two of the available quantitative MR-based techniques to assess microscopic tissue damage [Filippi et al., 2004; Ingle et al., 2002; Miller and Leary, 2007]. As a consequence, we can not rule out that the application of other methods, such as ^{1}H-MRS, which can reliable assess other important pathological substrates of the disease (e.g., axonal damage/dysfunction) [De Stefano and Filippi, 2007], might improve our ability of detecting such a correlation. However, the ^{1}H-MRS resolution at a voxel-level is relatively poor [De Stefano and Filippi, 2007]. Third, despite our effort to have a precise location of brain tissue damage, we used a relatively rough scale to measure clinical disability, and we did not assess impairment in clinical domains, including cognitive dysfunction. Indeed, a recent study [Kragt et al., 2008] demonstrated a limited value of EDSS in the assessment of PPMS patients, which prompts the application of more accurate and sophisticated clinical scales, at least in this patient subgroup. Nevertheless, we can not exclude that the volumetry and diffusivity abnormalities that we detected might precede the appearance of clinical symptoms. In this perspective, only a longitudinal study might help to shed light on this issue.

CONCLUSIONS

A multiparametric assessment of regional distribution of damage in different brain compartments may be a valuable tool to improve the understanding of the mechanisms related to the accumulation of irreversible disability in PPMS.

Clearly, our study is not without limitations. First, the sample size is relatively small, and, as a consequence, the extent of GM involvement might have been underestimated. Second, although the use of a relatively large smoothing kernel and small cluster size may have

decreased the possibility to detect small changes in GM structure, a thresholded map was applied to increase the certainty that the abnormal regions were located in the GM and to avoid partial volume effects. Third, a cognitive evaluation was not planned for the patients involved in this study. Future studies, with a comprehensive assessment of involvement in different neurological systems should contribute to further define the relation between damage and dysfunction of specific regions.

REFERENCES

Agosta F, Benedetti B, Rocca MA, Valsasina P, Rovaris M, Comi G, Filippi M (2005): Quantification of cervical cord pathology in primary progressive MS using diffusion tensor MRI. Neurology 64:631–635.

Agosta F, Rovaris M, Pagani E, Sormani MP, Comi G, Filippi M (2006): Magnetization transfer MRI metrics predict the accumulation of disability 8 years later in patients with multiple sclerosis. Brain 129:2620–2627.

Agosta F, Absinta M, Sormani MP, Ghezzi A, Bertolotto A, Montanari E, Comi G, Filippi M (2007): In vivo assessment of cervical cord damage in MS patients: A longitudinal diffusion tensor MRI study. Brain 130:2211–2219.

Ashburner J, Friston KJ (2000): Voxel-based morphometry—The methods. NeuroImage 11:805–821.

Audoin B, Davies GR, Finisku L, Chard DT, Thompson AJ, Miller DH (2006): Localization of grey matter atrophy in early RRMS: A longitudinal study. J Neurol 253:1495–1501.

Brownell B, Hughes J (1962): The distribution of plaques in the cerebrum in multiple sclerosis. J Neurol Neurosurg Psychiatry 25:315–320.

Camp SJ, Stevenson VL, Thompson AJ, Ingle GT, Miller DH, Borras C, Brochet B, Dousset V, Falautano M, Filippi M, Kalkers NF, Montalban X, Polman CH, Langdon DW (2005): A longitudinal study of cognition in primary progressive multiple sclerosis. Brain 128:2891–2898.

Ceccarelli A, Rocca MA, Falini A, Tortorella P, Pagani E, Rodegher M, Comi G, Scotti G, Filippi M (2007): Normal-appearing white and grey matter damage in MS. A volumetric and diffusion tensor MRI study at 3.0 Tesla. J Neurol 254:513–518.

Ceccarelli A, Rocca MA, Pagani E, Ghezzi A, Capra R, Falini A, Scotti G, Comi G, Filippi M (2008): The topographical distribution of tissue injury in benign MS: A 3T multiparametric MRI study. NeuroImage 39:1499–509.

Ceccarelli A, Rocca MA, Pagani E, Colombo B, Martinelli V, Comi G, Filippi M (2008): A voxel-based morphometry study of grey matter loss in MS patients with different clinical phenotypes. NeuroImage 42:315–322.

Charil A, Filippi M, Falini A (2006):High-field strength MRI (3.0 T or more) in white matter diseases. In: Scarabino T, Salvolini U, editors. High Field Brain MRI-Use in Clinical Practice. Berlin: Springer.186–193.

Cifelli A, Arridge M, Jezzard P, Esiri MM, Palace J, Matthews PM (2002): Thalamic neurodegeneration in multiple sclerosis. Ann Neurol 52:650–653.

De Stefano N, Filippi M (2007): MR spectroscopy in multiple sclerosis. J Neuroimaging 17:31S–35S.

Ehrsson HH, Kuhtz-Buschbeck JP, Forssberg H (2002): Brain regions controlling nonsynergistic versus synergistic movement of the digits: A functional magnetic resonance imaging study. J Neurosci 22:5074–5080.

Fabiano AJ, Sharma J, Weinstock-Guttman B, Munschauer FE III, Benedict RH, Zivadinov R, Bakshi R (2003): Thalamic involvement in multiple sclerosis: A diffusion-weighted magnetic resonance imaging study. J Neuroimaging 13:307–314.

Farrell JA, Landman BA, Jones CK, Smith SA, Prince JL, van Zijl PC, Mori S (2007): Effects of SNR on the accuracy and reproducibility of DTI derived fractional anisotropy, mean diffusivity, and principal eigenvector measurements at 1.5T. J Magn Reson Imaging 26:756–767.

Filippi M, Inglese M, Rovaris M, Sormani MP, Horsfield P, Iannucci PG, Colombo B, Comi G (2000): Magnetization transfer imaging to monitor the evolution of MS: A 1-year follow-up study. Neurology 55:940–946.

Filippi M, Rovaris M, Rocca MA (2004): Imaging primary progressive multiple sclerosis: The contribution of structural, metabolic, and functional MRI techniques. Mult Scler 10:36–44.

Galanaud D, Nicoli F, Le Fur Y, Guye M, Ranjeva JP, Confort-Gouny S, Viout P, Soulier E, Cozzone PJ (2003): Multimodal magnetic resonance imaging of the central nervous system. Biochimie 85:905–914.

Good CD, Johnsrude IS, Ashburner J, Henson RN, Friston KJ, Frackowiak RS (2001): Avoxel-based morphometric study of ageing in 465 normal adult human brains. NeuroImage 14:21–36.

Iannucci G, Iannucci G, Rovaris M, Giacomotti L, Comi G, Filippi M (2001): Correlation of multiple sclerosis measures derived from T2-weighted, T1-weighted,magnetization transfer, and diffusion tensor MR imaging. AJNR Am J Neuroradiol 22: 1462–1467.

Ingle GT, Thompson AJ, Miller DH (2002): Magnetic resonance imaging in primary progressive multiple sclerosis. J Rehabil Res Dev 39:261–271.

Inglese M, Liu S, Babb JS, Mannon LJ, Grossman RI, Gonen O (2004): Three-dimensional proton spectroscopy of deep gray matter nuclei in relapsing-remitting MS. Neurology 63:170–172.

Inglese M, Park SJ, Johnson G, Babb JS, Miles L, Jaggi H, Herbert J, Grossman RI (2007): Deep gray matter perfusion in multiple sclerosis: Dynamic susceptibility contrast perfusion magnetic resonance imaging at 3T. Arch Neurol 64:196–202.

Khaleeli Z, Cercignani M, Audoin B, Ciccarelli O, Miller DH, Thompson AJ (2007): Localized grey matter damage in early primary progressive multiple sclerosis contributes to disability. NeuroImage 37:253–261.

Kragt JJ, Thompson AJ, Montalban X, Tintoré M, Río J, Polman CH, Uitdehaag BM (2008): Responsiveness and predictive value of EDSS and MSFC in primary progressive MS. Neurology 70:1084–1091.

Kurtzke JF (1983): Rating neurologic impairment in multiple sclerosis: An expanded disability status scale (EDSS). Neurology 33:1442–1452.

Kutzelnigg A, Lucchinetti CF, Stadelmann C, Bruek W, Rauschka H, Bergmann M, Schmidbauer M, Parisi JE, Lassmann H (2005): Cortical demyelination and diffuse white matter injury in multiple sclerosis. Brain 128:2705–2712.

Lassmann H, Brück W, Lucchinetti CF (2007): The immunopathology of multiple sclerosis: An overview. Brain Pathol 17:210–218.

Mainero C, De Stefano N, Iannucci G, Sormani MP, Guidi L, Federico A, Bartolozzi ML, Comi G, Filippi M (2001): Correlates of MS disability assessed in vivo using aggregates of MR quantities. Neurology 56:1331–1334.

Mesaros S, Rocca MA, Absinta M, Ghezzi A, Milani N, Moiola L, Veggiotti P, Comi G, Filippi M (2008): Evidence of thalamic gray matter loss in pediatric multiple sclerosis. Neurology 70:1107–1112.

Miller DH, Leary SM (2007): Primary-progressive multiple sclerosis. Lancet Neurol 6:903–912.

Ormerod IE, Miller DH, McDonald WI, du Boulay EP, Rudge P, Kendall BE, Moseley IF, Johnson G, Tofts PS, Halliday AM, Bronstein AM, Scaravilli F, Harding AE, Barnes D, Zilkha KJ (1987): The role of NMR imaging in the assessment of multiple sclerosis and isolated neurological lesions. A quantitative study. Brain 110:1579–1616.

Pagani E, Filippi M, Rocca MA, Horsfield MA (2005): A method for obtaining tract-specific diffusion tensor MRI measurements in the presence of disease: Application to patients with clinically isolated syndromes suggestive of multiple sclerosis. NeuroImage 26:258–265.

Paulesu E, Perani D, Fazio F, Comi G, Pozzilli C, Martinelli V, Filippi M, Bettinardi V, Sirabian G, Passafiume D, Anzini A, Lenzi GL, Canal N, Fieschi C (1996): Functional basis of memory impairment in multiple sclerosis: A [18F] FDG PET study. NeuroImage 4:87–96.

Pierpaoli C, Basser PJ (1996): Toward a quantitative assessment of diffusion anisotropy. Magn Reson Med 36:893–906.

Polman CH, Reingold SC, Edan G, Filippi M, Hartung HP, Kappos L, Lublin FD, Metz LM, McFarland HF, O'Connor PW, Sandberg-Wollheim M, Thompson AJ, Weinshenker BG, Wolinsky JS (2005): Diagnostic criteria for multiple sclerosis: 2005 revisions to the McDonald Criteria. Ann Neurol 58:840–846.

Rocca MA, Iannucci G, Rovaris M, Comi G, Filippi M (2003): Occult tissue damage in patients with primary progressive multiple sclerosis is independent of T2-visible lesions—A diffusion tensor MR study. J Neurol 250:456–460.

Rovaris M, Bozzali M, Santuccio G, Ghezzi A, Caputo D, Montanari E, Bertolotto A, Bergamaschi R, Capra R, Mancardi G, Martinelli V, Comi G, Filippi M (2001): In vivo assessment of the brain and cervical cord pathology of patients with primary progressive multiple sclerosis. Brain 124:2540–2549.

Rovaris M, Bozzali M, Iannucci G, Ghezzi A, Caputo D, Montanari E, Bertolotto A, Bergamaschi R, Capra R, Mancardi GL, Martinelli V, Comi G, Filippi M (2002): Assessment of normal-appearing white and gray matter in patients with primary progressive multiple sclerosis: A diffusion-tensor magnetic resonance imaging study. Arch Neurol 59:1406–1412.

Rovaris M, Gallo A, Falini A, Benedetti B, Rossi P, Comola M, Scotti G, Comi G, Filippi M (2005a): Axonal injury and overall tissue loss are not related in primary progressive multiple sclerosis. Arch Neurol 62:898–902.

Rovaris M, Gallo A, Valsasina P, Benedetti B, Caputo D, Ghezzi A, Montanari E, Sormani MP, Bertolotto A, Mancardi G, Bergamaschi R, Martinelli V, Comi G, Filippi M (2005b): Short-term accrual of gray matter pathology in patients with progressive multiple sclerosis: An in vivo study using diffusion tensor MRI. NeuroImage 24:1139–1146.

Rovaris M, Judica E, Sastre-Garriga J, Rovira A, Sormani MP, Benedetti B, Korteweg T, De Stefano N, Khaleeli Z, Montalban X, Barkhof F, Miller DH, Polman C, Thompson A, Filippi M (2008): Large-scale, multicentre, quantitative MRI study of brain and cord damage in primary progressive multiple sclerosis. Mult Scler 14:455–464.

Schmahmann JD, Sherman JC (1998): The cerebellar cognitive affective syndrome. Brain 121:561–579.

Schmahmann JD, Caplan D (2006): Cognition, emotion and the cerebellum. Brain 129:290–292.

Sepulcre J, Sestre-Garriga J, Cercignani M, Ingle GT, Miller DH, Thomspon AJ (2006): Regional gray matter atrophy in early primary progressive multiple sclerosis: A voxel-based morphometry study. Arch Neurol 63:1175–1180.

Sepulcre J, Masdeu JC, Sastre-Garriga J, Goñi J, Vélez-de-Mendizábal N, Duque B, Pastor MA, Bejarano B, Villoslada P (2008): Mapping the brain pathways of declarative verbal memory: Evidence from white matter lesions in the living human brain. NeuroImage 42:1237–1243.

Smith SM, De Stefano N, Jenkinson M, Matthews PM (2001): Normalized accurate measurement of longitudinal brain change. J Comput Assist Tomogr 25:466–475.

Thompson AJ, Montalban X, Barkhof F, Brochet B, Filippi M, Miller DH, Polman CH, Stevenson VL, McDonald WI (2000): Diagnostic criteria for primary progressive multiple sclerosis: A position paper. Ann Neurol 47:831–835.

Wylezinska M, Cifelli A, Jezzard P, Palace J, Alecci M, Matthews PM (2003): Thalamic neurodegeneration in relapsing-remitting multiple sclerosis. Neurology 60:1949–1954.